

# Formation of Dianions in Helium Nanodroplets\*\*

Andreas Mauracher, Matthias Daxner, Stefan E. Huber, Johannes Postler, Michael Renzler, Stephan Denifl, Paul Scheier,\* and Andrew M. Ellis\*

**Abstract:** The formation of dianions in helium nanodroplets is reported for the first time. The fullerene cluster dianions  $(C_{60})_n^{2-}$  and  $(C_{70})_n^{2-}$  were observed by mass spectrometry for  $n \geq 5$  when helium droplets containing the appropriate fullerene were subjected to electron impact at approximately 22 eV. A new mechanism for dianion formation is described, which involves a two-electron transfer from the metastable  $He^-$  ion. As well as the prospect of studying other dianions at low temperature using helium nanodroplets, this work opens up the possibility of a wider investigation of the chemistry of  $He^-$ , a new electron-donating reagent.

**M**ultiply charged anions (MCAs) are common constituents of chemical systems. However, when stripped of a counterion and/or solvent the Coulomb repulsion between the two or more excess electrons usually makes the anion unstable with respect to processes such as electron autodetachment or fission into singly charged anions (Coulomb explosion).<sup>[1–3]</sup> For this reason the study of isolated MCAs in the gas phase has proved a major experimental challenge.

Nevertheless, MCAs have been detected in the gas phase in the past few decades. The earliest examples were certain large organic dianions, derived from substituted polyaromatic hydrocarbons, which are favorable because the excess negative charge can be distributed over a substantial volume, thus minimizing electrostatic repulsion.<sup>[4]</sup> More recently a variety of specialized techniques have been employed to generate MCAs in the gas phase. For example, surface sputtering using highly energetic cations as projectiles has yielded  $C_n^{2-}$  ions, where  $n \geq 7$ ,<sup>[5]</sup> whereas laser desorption has been used to form the fullerene dianions  $C_{60}^{2-}$  and  $C_{70}^{2-}$ .<sup>[6,7]</sup> Other important developments include the production of dianions and trianions of large metal clusters, including those of silver, gold, and lead.<sup>[8–10]</sup> These anions were made by using laser ablation to generate monoanions, which were then isolated in a Penning trap and flooded with low-energy electrons to make MCAs. Electrospray ionization is also a source of solvent-free MCAs,

and examples studied include the carbon cluster dianions  $C_{84}^{2-}$  and  $C_{90}^{2-}$ ,<sup>[11]</sup> the citrate dianions,<sup>[12]</sup> and a variety of dicarboxylate dianions of formula  $[OOC(CH_2)_nCOO]^{2-}$ .<sup>[13]</sup>

Herein we report the first observation of dianions produced in liquid helium nanodroplets. The focus of the current study is on dianions of  $C_{60}$  and  $C_{70}$  clusters. Aside from this original observation, there are two important underlying aspects of this work. First, we demonstrate a new method for producing and studying dianions, which may be applicable to MCAs beyond those covered in this paper. Second, evidence is presented for a new and unusual mechanism, which accounts for the formation of dianions in helium nanodroplets.

Figure 1 a) shows a negative-ion mass spectrum obtained at an electron energy of 22 eV for helium droplets doped with  $C_{60}$ . The dominant peaks in this mass spectrum arise from the monoanions  $(C_{60})_n^-$ , which form a clear series. The production of monoanions in the gas phase from electron attachment to doped helium nanodroplets is already well known.<sup>[14,15]</sup>

Much weaker are additional peaks in the spectrum (Figure 1 a) between  $m/z$  2000 and 6000, which are precisely mid-way between the intense  $(C_{60})_n^-$  peaks and are assigned

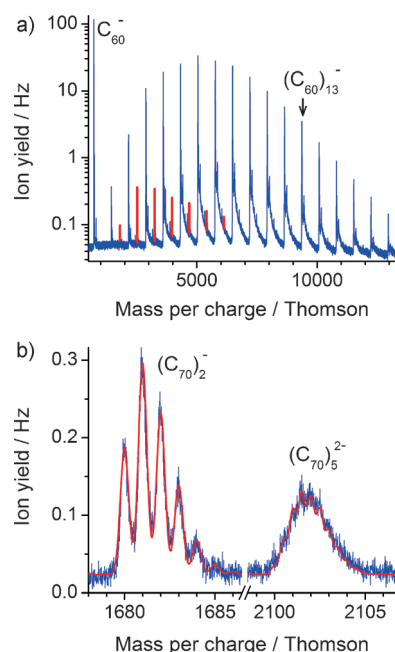


**Figure 1.** a) Survey mass spectrum showing dominant peaks from  $(C_{60})_n^-$  anions. The weaker features marked in red arise from  $(C_{60})_n^{2-}$  dianions. Note the logarithmic vertical scale. b) An expanded view of the mass spectrum from  $C_{70}$  clusters focusing on two specific anions,  $(C_{70})_2^-$  and  $(C_{70})_5^-$ . Also shown (in red) is a simulation of the isotope structure based on natural isotope abundances.

[\*] A. Mauracher, M. Daxner, S. E. Huber, J. Postler, M. Renzler, S. Denifl, P. Scheier  
Institut für Ionenphysik und Angewandte Physik  
Universität Innsbruck  
Technikerstr. 25, 6020 Innsbruck (Austria)  
E-mail: Paul.Scheier@uibk.ac.at

A. M. Ellis  
Department of Chemistry, University of Leicester  
University Road, Leicester, LE1 7RH (UK)  
E-mail: andrew.ellis@le.ac.uk

[\*\*] This work was given financial support by the Austrian Science Fund (FWF), Wien (P23657, P24443, and I978).

Supporting information for this article is available on the WWW under <http://dx.doi.org/10.1002/ange.201408172>.

to the dianions,  $(C_{60})_n^{2-}$ . As another illustration, Figure 1b shows an expanded spectrum derived from  $C_{70}$ . As well as peaks attributed to  $(C_{70})_2^-$ , a broad feature at the expected position for  $(C_{70})_5^{2-}$  is seen. Simulations of the isotope structure based on a statistical distribution of  $^{12}\text{C}$  and  $^{13}\text{C}$  are also presented and are fully consistent with the assignments, thus providing unequivocal confirmation of dianion formation. The smallest observable dianion cluster corresponds to  $n=5$  for both  $C_{60}$  and  $C_{70}$ .

How can  $(C_{60})_n^{2-}$  ions form in helium nanodroplets? This question is important because there is no existing mechanism in the literature that accounts for this. Sequential electron attachment can be ruled out because of the strong Coulombic repulsion after addition of the first electron. However, as will be argued shortly, the definitive proof comes from the dependence of the dianion signal on the incoming electron kinetic energy, which is shown in Figure 2. The upper panel

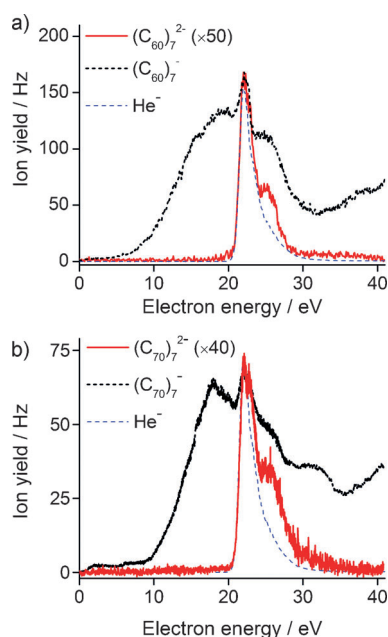


**Figure 2.** a) Comparison of anion yield curves as a function of incident electron kinetic energy for  $\text{He}^-$ ,  $(C_{60})_7^-$ , and  $(C_{60})_7^{2-}$ . b) Parts of the anion yield curves for  $\text{He}^-$ ,  $(C_{70})_7^-$ , and  $(C_{70})_7^{2-}$ . The yield curves for both  $\text{He}^-$  and the fullerene cluster dianions are asymmetric, which is attributed to the production of  $\text{He}^-$  in states above the lowest  $^4\text{P}$  state. The more pronounced asymmetry for the dianion curves suggests that the excited states are more reactive than the lowest state of  $\text{He}^-$ .

includes the yield curve of a selected monoanion,  $(C_{60})_7^-$ , together with that of the corresponding dianion,  $(C_{60})_7^{2-}$ . Note that the dianion signal is much weaker than that of the corresponding monoanion, so that the dianion trace in Figure 2a has been enlarged to facilitate a comparison. To interpret the fullerene cluster ion yield curves, we first need to consider another ion yield curve, namely that of  $\text{He}^-$  (Figure 2a).

$\text{He}^-$  has been known for some time in the gas phase but has only recently been reported as a product from electron impact on helium droplets.<sup>[16]</sup> Formation of  $\text{He}^-$  requires electronic excitation, as ground-state atomic helium has

a negative electron affinity and so cannot attach an electron.  $\text{He}^-$  can be formed from the first excited metastable state of He, the  $1s2s\ ^3\text{S}_1$  state, at 19.8 eV.<sup>[17]</sup> In helium droplets, approximately 1.2 eV of additional energy is required for the electron to penetrate the droplet and form a cavity (“bubble”) after the inelastic scattering event.<sup>[16]</sup> Thus at approximately 21 eV, the  $^3\text{S}_1$  state of He, or  $\text{He}^*$  in shorthand notation, along with a slow electron from the inelastic scattering of the original incoming electron, can form. This slow electron can then attach to  $\text{He}^*$  to make  $\text{He}^{*-}$ , which we write as  $\text{He}^-$  from here onwards. However, in helium droplets doped with molecules, the  $\text{He}^*$  competes with the dopant in attracting the slow electron, and in relatively small droplets, the dopant usually wins because of its higher polarizability than  $\text{He}^*$  and thus attracts the electron through a stronger charge-induced dipole interaction (plus electrostatic interactions where appropriate). Only when the droplets are sufficiently large ( $\geq 10^5$  helium atoms<sup>[16]</sup>), allowing  $\text{He}^*$  to be made at a considerable distance from any dopant, can  $\text{He}^-$  form.  $\text{He}^-$  occupies a bubble because of strong repulsive interactions with neighboring helium atoms.

$\text{He}^-$  is metastable, with a lifetime depending on the state occupied, but the longest lived is the  $1s2s2p\ ^4\text{P}_{5/2}$  state with a lifetime of 365  $\mu\text{s}$  in the gas phase.<sup>[18]</sup> The short lifetime makes it difficult to study reactive collisions of  $\text{He}^-$  in the gas phase, and no such studies have been reported thus far. However, if the  $\text{He}^-$  bubble travels at the Landau velocity for superfluid  $^4\text{He}$  (ca. 60  $\text{m s}^{-1}$ ), then it can traverse a droplet of the size employed in the current work in  $< 1$  ns. In fact, the available experimental evidence suggests that the lifetime of  $\text{He}^-$  in helium droplets is much longer than in the gas phase.<sup>[16]</sup> Thus, once formed,  $\text{He}^-$  will be attracted to a molecular dopant and has ample time to react.

The yield curves for the monoanions and dianions selected for illustration in Figure 2a,  $(C_{60})_7^-$  and  $(C_{60})_7^{2-}$ , differ dramatically. On the other hand, the yield curves for  $\text{He}^-$  and  $(C_{60})_7^{2-}$  are similar and show a relatively narrow resonance peaking near 22 eV. Given the overwhelming similarities of their anion yield curves, the  $(C_{60})_n^{2-}$  anions must be formed by a two-electron transfer from  $\text{He}^-$ , a new means of preparing dianions. Figure 2b is similar to 2a but shows data for  $C_{70}$  clusters. Again the similarity between the ion yield curves for  $(C_{70})_7^{2-}$  and  $\text{He}^-$  is striking, showing that the  $(C_{70})_n^{2-}$  dianions also derive from double electron transfer from  $\text{He}^-$ .

Both the  $\text{He}^-$  and fullerene cluster dianion yield curves are asymmetric and have underlying structure. This is seen most clearly in the  $(C_{70})_n^{2-}$  curve in Figure 2b, where a second peak lies approximately 1 eV above the strongest peak: Indeed, the asymmetry continues to higher energies, presumably because other weak and unresolved peaks contribute. These additional peaks are consistent with production of  $\text{He}^-$  in various metastable excited electronic states lying above the lowest observed state ( $1s2s2p\ ^4\text{P}$ ). For example, the  $1s2p\ ^3\text{P}$  state of neutral He is 1.14 eV above the  $1s2s\ ^3\text{S}$  state,<sup>[19]</sup> and an electron attached to the former would be consistent with the second peak in both the  $\text{He}^-$  and fullerene dianion yield curves. However, the asymmetry is far more prominent in the case of the dianion curves than in the  $\text{He}^-$  curve, and we

attribute this feature to the enhanced reactivity of the more highly electronically excited  $\text{He}^-$  ions.

To assess the energetic viability of a two-electron transfer from  $\text{He}^-$  to a fullerene cluster, we first considered the  $\text{C}_{60}$  monomer. The dianion,  $\text{C}_{60}^{2-}$ , has been observed previously in experiments and appears to be metastable with respect to the monoanion and a free electron.<sup>[6,7,20,21]</sup> The first adiabatic electron affinity of  $\text{C}_{60}$  has been determined experimentally as  $2.6835 \pm 0.0006$  eV.<sup>[22]</sup> The second electron affinity of  $\text{C}_{60}$  has not been measured, but a theoretical estimate puts it close to  $-0.4$  eV,<sup>[23]</sup> and this negative value is consistent with the reported metastability of  $\text{C}_{60}^{2-}$ . Given that the first ionization energy of He is 24.56 eV and the electronic excitation energy contained within the lowest state of  $\text{He}^-$  is approximately 19.7 eV, the energetic deficit is 2.6 eV.  $\text{C}_{60}^{2-}$  should therefore not be produced in a low-temperature collision between  $\text{C}_{60}$  and the lowest metastable state of  $\text{He}^-$ , which is consistent with our experiments. A similar conclusion can be reached for  $\text{C}_{70}$  on the basis of reported electron affinities.<sup>[23]</sup>

The double electron affinities of  $(\text{C}_{60})_n$  and  $(\text{C}_{70})_n$  clusters should be larger than those of the monomers because a more diffuse excess-electron distribution is possible. The only reported value for the double electron affinity of a  $(\text{C}_{60})_n$  cluster is an estimate of 3.86 eV for  $(\text{C}_{60})_2$  from some relatively crude ab initio calculations.<sup>[24]</sup> Given the lack of electron affinity data for fullerene clusters, we have performed DFT calculations on  $(\text{C}_{60})_n$  clusters and their anions for  $n = 1-5$  as part of this work, and Figure 3 summarizes the

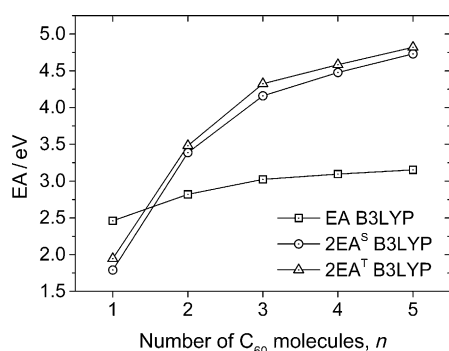


**Figure 3.** Single and double vertical electron affinities (designated as EA and 2EA) of  $(\text{C}_{60})_n$  clusters as determined from DFT calculations (B3LYP/6-31 + G(d)). The calculated electron affinities for both  $\text{C}_{60}$  and  $(\text{C}_{60})_2$  are insensitive to modest changes in geometry, and so the adiabatic and vertical electron affinities are likely to be comparable. The double electron affinity curves for singlet ( $2\text{EA}^{\text{S}}$ ) and triplet ( $2\text{EA}^{\text{T}}$ ) states of the dianion are also shown and very similar.

findings graphically. The addition of two electrons can create a singlet or triplet dianion, but the electron affinities are not affected significantly by the spin state, so this can be ignored. As Figure 3 shows, the second electron affinity for  $n \geq 2$  is calculated to be positive, and at around  $n = 4$ , the formation of the dianion becomes thermodynamically allowed in a two-electron transfer from  $\text{He}^-$ .

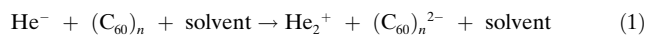
The mechanism by which  $\text{He}^-$  transfers its two loosely bound electrons to the dopant remains to be determined. In particular, is it a two-step reduction or a concerted two-

electron process? A clue can be found in the anion yield curves in Figure 2. The curves for the  $(\text{C}_{60})_7^-$  and  $(\text{C}_{70})_7^-$  monoanions, which are typical of those of other  $(\text{C}_{60})_n^-$  and  $(\text{C}_{70})_n^-$  ions, are broad and consistent with direct electron attachment as the main source of monoanions. In a sequential two-electron transfer from  $\text{He}^-$ , one might occasionally expect the second step to fail, delivering a peak at approximately 22 eV in the monoanion yield curve matching that of the lowest  $\text{He}^-$  resonance. A small peak is seen at 22 eV for the monoanion signals shown in Figure 2 but the equivalent peak is absent for cluster monoanions with  $n > 7$ . The absence of the 22 eV peak for the monoanions of larger clusters suggests that this peak is the result of some instability of the smaller cluster dianions with respect to Coulomb explosion, leading to monoanions such as  $(\text{C}_{60})_7^-$  and  $(\text{C}_{70})_7^-$ . The evidence therefore suggests that dianions derive from a concerted two-electron transfer from  $\text{He}^-$ . A single-step two-electron transfer also avoids the challenge of overcoming the Coulomb repulsion in the second step of a sequential electron transfer mechanism.

A concerted two-electron transfer is consistent with the strong electron correlation expected between the outermost electrons in doubly excited electronic states. In negatively charged doubly excited ions, this effect is accentuated by the excess negative charge, which shields the excited electrons from the nuclear charge and often results in electron correlation providing the majority of the electron binding energy.<sup>[25,26]</sup>

However, after transfer of the two electrons, the cation and dianion must overcome Coulomb attraction to separate. A possibility is that electron transfer is a long-range process. On the basis of plausible assumptions about the double electron affinities of the fullerene clusters, together with the two-electron ionization energy of  $\text{He}^-$  (ca. 5 eV), we can use a simple harpoon model to estimate that two-electron transfer is possible at distances between the  $\text{He}^-$  and the fullerene cluster in excess of 10 Å. As the  $\text{He}^+$  is then dragged through the droplet towards the fullerene dianion,  $\text{He}_2^+$  can form. As the dissociation energy ( $D_e$ ) of  $\text{He}_2^+$  is near to 2.5 eV,<sup>[27]</sup> the kinetic energy release from forming this cation could allow the cation and dianion to separate.

To summarize, dianions derived from doped helium nanodroplets have been detected for the first time. These anions are formed by a new mechanism, concerted double electron transfer from  $\text{He}^-$ , an exotic entity formed in liquid helium at electron impact energies near 22 eV. This process is represented by the reaction:



where the solvent here is liquid helium (a video illustration of the mechanism of reaction (1) is provided in the Supporting Information). In this study,  $(\text{C}_{60})_n^{2-}$  and  $(\text{C}_{70})_n^{2-}$  ions were observed but the method used should be transferable to other types of dianions, both in isolation and in combination with other molecules, such as water. More generally this work will open the way for a wider study of the chemistry of  $\text{He}^-$ , a new electron donor.

## Experimental Section

Helium nanodroplets were produced by expanding high-purity gaseous helium at a stagnation pressure of 24 bar and a temperature of 9.6 K through a 5  $\mu\text{m}$  pinhole into a vacuum. Under these conditions the average number of helium atoms per droplet was in the region of  $3 \times 10^5$ . The expansion was skimmed to form a collimated droplet beam, and this was then passed through a heated pick-up cell containing either  $\text{C}_{60}$  or  $\text{C}_{70}$  (SES Research, purity 99.95 % and 99 %, respectively). After the pick-up of fullerene molecules from the vapor produced in the oven, the droplets passed through a skimmer to enter another differentially pumped chamber, where they were exposed to an electron beam of variable energy (0–150 eV). Any ions produced were then extracted into a high-resolution and high-repetition-rate reflectron time-of-flight mass spectrometer (Tofwerk).

Received: August 12, 2014

Published online: October 8, 2014

**Keywords:** density functional calculations · doubly charged anions · electron transfer · fullerenes · helium nanodroplets

- [1] M. K. Scheller, R. N. Compton, L. S. Cederbaum, *Science* **1995**, 270, 1160.
- [2] A. I. Boldyrev, M. Gutowski, J. Simons, *Acc. Chem. Res.* **1996**, 29, 497.
- [3] A. Dreuw, L. S. Cederbaum, *Chem. Rev.* **2002**, 102, 181.
- [4] R. C. Dougherty, *J. Chem. Phys.* **1969**, 50, 1896.
- [5] S. Schauer, P. Williams, R. N. Compton, *Phys. Rev. Lett.* **1990**, 65, 625.
- [6] R. L. Hettich, R. N. Compton, R. H. Ritchie, *Phys. Rev. Lett.* **1991**, 67, 1242.
- [7] P. A. Limbach, L. Schweikhard, K. A. Cowen, M. T. McDermott, A. G. Marshall, J. V. Coe, *J. Am. Chem. Soc.* **1991**, 113, 6795.
- [8] A. Herlert, S. Krückberg, L. Schweikhard, M. Vogel, C. Walther, *Phys. Scr.* **1999**, T80, 200.
- [9] C. Stoermer, J. Friedrich, M. M. Kappes, *Int. J. Mass Spectrom.* **2001**, 206, 63.
- [10] C. Yannouleas, U. Landman, A. Herlert, L. Schweikhard, *Phys. Rev. Lett.* **2001**, 86, 2996.
- [11] G. Khairallah, J. B. Peel, *Chem. Phys. Lett.* **1998**, 296, 545.
- [12] X. B. Wang, C. F. Ding, L. S. Wang, *Phys. Rev. Lett.* **1998**, 81, 3351.
- [13] L. S. Wang, C. F. Ding, X. B. Wang, J. B. Nicholas, *Phys. Rev. Lett.* **1998**, 81, 2667.
- [14] S. Denifl, F. Zappa, I. Mähr, J. Lecointre, M. Probst, T. D. Märk, P. Scheier, *Phys. Rev. Lett.* **2006**, 97, 043201.
- [15] F. Zappa, S. Denifl, I. Mähr, A. Bacher, O. Echt, T. D. Märk, P. Scheier, *J. Am. Chem. Soc.* **2008**, 130, 5573.
- [16] A. Mauracher, M. Daxner, J. Postler, S. E. Huber, S. Denifl, P. Scheier, J. P. Toennies, *J. Phys. Chem. Lett.* **2014**, 5, 2444.
- [17] P. Kristensen, U. V. Pedersen, V. V. Petrunin, T. Anderson, K. T. Chung, *Phys. Rev. A* **1997**, 55, 978.
- [18] U. V. Pedersen, M. Hyde, S. P. Möller, T. Anderson, K. T. Chung, *Phys. Rev. A* **2001**, 64, 012503.
- [19] A. Kramida, Y. Ralchenko, J. Reader, and NIST ASD Team (2012). *NIST Atomic Spectra Database* (version 5.0). Available from <http://physics.nist.gov/asd> [Tuesday, 10-Sep-2013 11:47:31 EDT]. National Institute of Standards and Technology, Gaithersburg, MD.
- [20] B. Liu, P. Hvelplund, S. B. Nielsen, S. Tomita, *Phys. Rev. Lett.* **2004**, 92, 168301.
- [21] S. Tomita, J. U. Andersen, H. Cederquist, B. Concina, O. Echt, J. S. Forster, K. Hansen, B. A. Huber, P. Hvelplund, J. Jensen, B. Liu, B. Manil, L. Manoury, S. Brønsted Nielsen, J. Rangama, H. T. Schmidt, H. Zettergren, *J. Chem. Phys.* **2006**, 124, 024310.
- [22] D.-L. Huang, P. D. Dau, H.-T. Liu, L.-S. Wang, *J. Chem. Phys.* **2014**, 140, 224315.
- [23] H. Zettergren, M. Alcamí, F. Martín, *Phys. Rev. A* **2007**, 76, 043205.
- [24] K. H. Lee, H. M. Lee, W. R. Lee, S. S. Park, H. Lee, T. Y. Park, X. Sun, K. Nasu, *Synth. Met.* **1997**, 86, 2389.
- [25] T. Andersen, *Phys. Rep.* **2004**, 394, 157.
- [26] D. J. Pegg, *Rep. Prog. Phys.* **2004**, 67, 857.
- [27] C. W. Bauschlicher, Jr., H. Partridge, *Chem. Phys. Lett.* **1989**, 160, 183.